AIP | Applied Physics Letters

Electronic and magnetic properties of La2NiMnO6 and La2CoMnO6 with cationic ordering

Min Zhu, Yong Lin, Edward W. C. Lo, Qiong Wang, Zhengjie Zhao et al.

Citation: Appl. Phys. Lett. **100**, 062406 (2012); doi: 10.1063/1.3683550
View online: http://dx.doi.org/10.1063/1.3683550
View Table of Contents: http://apl.aip.org/resource/1/APPLAB/v100/i6
Published by the American Institute of Physics.

Electronic and magnetic properties of La_2NiMnO_6 and La_2CoMnO_6 with cationic ordering

Min Zhu,[1,a)] Yong Lin,[2] Edward W. C. Lo,[2] Qiong Wang,[1] Zhengjie Zhao,[1] and Wenhui Xie[1,b)]
[1]*Engineering Research Center for Nanophotonics and Advanced Instrument, Department of Physics, East China Normal University, Shanghai 200062, China*
[2]*Department of Electrical Engineering, The Hong Kong Polytechnic University, Hung Hom, Kowloon, Hong Kong*

(Received 11 November 2011; accepted 21 January 2012; published online 10 February 2012)

Employing first-principles electronic structure calculations, the electronic and magnetic properties of La_2NiMnO_6 and La_2CoMnO_6 with Ni/Mn and Co/Mn ordering in (001), (110), and (111) directions are investigated. The ground states of La_2NiMnO_6 and La_2CoMnO_6 are ferromagnetic semiconducting with alternative Ni/Mn and Co/Mn ordering along the (111) direction. Furthermore, it is found that La_2NiMnO_6 and La_2CoMnO_6 are half-metal with Ni/Mn or Co/Mn ordering along (001) and (110) after considering the effect of electronic correlation. Our results would be helpful in exploring more spintronics materials. © *2012 American Institute of Physics*. [doi:10.1063/1.3683550]

Room-temperature semiconducting ferromagnet and half-metallic magnetic materials attract significant scientific attention due to their great potential application in spintronic devices.[1,2] Double perovskite La_2NiMnO_6 (LNMO) and La_2CoMnO_6 (LCMO) are attractive due to their impressive properties and potential on industrial applications.[3–13] LNMO is a ferromagnetic semiconductor with high critical temperature of $T_c \approx 280$ K, which may be used in commercial solid-state thermoelectric (Peltier) coolers.[3] LCMO is also a ferromagnetic semiconductor with critical temperature $T_c \approx 230$ K.[4,9] Several crystal structures have been identified, and it is confirmed that the ferromagnetic semiconductors LNMO and LCMO with high T_c are $P2_1/n$ monoclinic structure, in which octahedra with Ni (or Co) and Mn centers alternately stacking along (111). Recent reports indicate LNMO and LCMO have considerable magnetodielectric effects at room temperature, which is very useful for future electronic device.[1–5]

LNMO thin films have been grown on different substrates, such as $NdGaO_3$ (110), $SrTiO_3$ (100), $LaAlO_3$ (100), and MgO (100).[14–18] Meanwhile, LCMO thin films can be grown on cubic (001) $SrTiO_3$ substrates by pulsed laser deposition.[19] Either in the form of bulk or films, local Co/Mn or Ni/Mn disorder has been observed which results in the coexistence of multi phases with various behaviors.[3–10] The distinct disorder effects in LNMO and LCMO thus call for the first-principle investigation for effect of cation ordering, but such kind of calculation does not exist. Furthermore, due to recent developments of molecular beam epitaxy (MBE) technology, perovskite oxides superlattices can be grown layer by layer with very high quality. Thus, it should be feasible to grow LNMO (LCMO) with Ni (Co) and Mn cations alternatively along (001), (110), and (111) with high atomic order. Therefore, it attracts more interest to investigate the effect of Co/Mn or Ni/Mn atomic ordering by first-principle investigation.

Six model structures are built with Ni/Mn or Co/Mn orderly stacking along (001), (110), and (111) directions (see Fig. 1), named as LNMO (001), LNMO (110), LNMO (111), LCMO (001), LCMO (110), and LCMO (111), respectively. For each model, besides ferromagnetic (FM) state, several typical antiferromagnetic (AFM) states are also considered, but only the stablest AFM state is directly discussed. The experimental value of $P2_1/n$ phase is adopted:[10] the lattice constants of LNMO are $a = 5.467$ Å, $b = 5.510$ Å, $c = 7.751$ Å, and $\beta = 91.12°$ and LCMO are $a = 5.525$ Å, $b = 5.488$ Å, $c = 7.779$ Å, and $\beta = 89.95°$. The electronic structure calculations were carried out using the plane wave pseudopotential method implemented within the Vienna *ab-initio* simulation package (VASP).[20] Generalized gradient approximation (GGA)[21] is used for exchange-correlation functionals. Electronic correlation effects are considered by using GGA + U (rotationally invariant approach) with $U_{eff} = 3$ eV for Mn, CO, and Ni, which are typical values used in the literature.[11–13] Projected augmented wave (PAW) potentials[22] were used, and the kinetic energy cutoff for expansion of wave functions was 400 eV. Reciprocal space integrations were carried out with a *k*-space mesh of $7 \times 7 \times 5$. The internal atomic coordinates are relaxed until force on each atom is smaller than 10 meV/Å.

Calculated total energy and magnetic moment are listed in Table I. It is found that FM state has the lowest energy for each atomic ordering structure of LNMO and LCMO, despite of tiny discrepancy of total energy between FM and AFM state of LNMO (110) with GGA and LCMO (110) with GGA + U. Both GGA and GGA + U calculations indicate that the total energy of FM states with (111) atomic order is the lowest for both LNMO and LCMO, which are consistent with experimental reports. The choice of U value would not change the ground state. The calculated magnetic moments of LNMO (111) and LCMO (111) FM state are in accordance with previous theoretical studies.[11–13] The

a)Min Zhu and Yong Lin contributed equally to this work.
b)Author to whom correspondence should be addressed. Electronic mail: whxie@phy.ecnu.edu.cn.

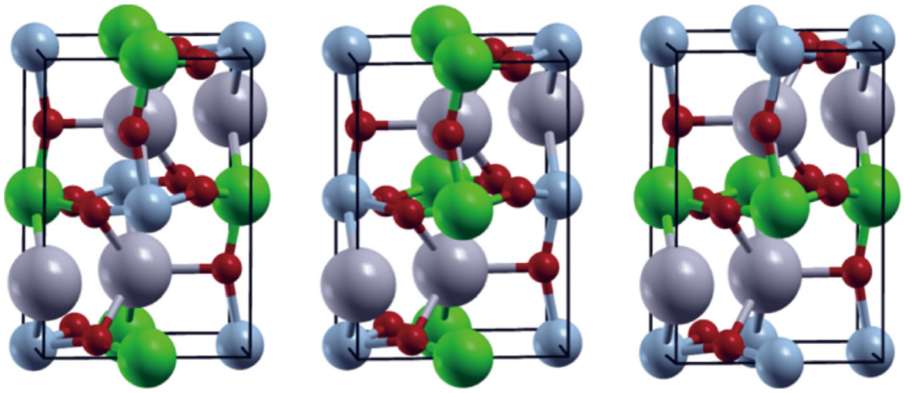

FIG. 1. (Color online) Three atomic model structures: (a) (111) order, (b) (110) order, and (c) (001) order. The red spheres are O (small size), blue spheres represent La (largest size), blue ones represent Ni/Co (middle size), and green ones represent Mn (big size).

magnetic moments of LNMO (001), LNMO (110), LCMO (001), and LCMO (110) FM states are not integer values in GGA calculations, slightly smaller than 5.0 μ_B/*f.u.* of LNMO and 6.0 μ_B/*f.u.* of LCMO in GGA + U calculations. AFM solutions with 1 μ_B net moment have parallel aligned Mn-O-Mn, Ni-O-Ni, or Co-O-Co linkage but antiparallel aligned Mn-O-Ni or Mn-O-Co linkage, so that the moment of Mn and Co (Ni) could not be offset. On the contrary, AFM solutions with zero net moment have antiparallel aligned Mn-O-Mn, Ni-O-Ni, or Co-O-Co linkage and parallel aligned Mn-O-Ni or Mn-O-Co linkage. The integer value of magnetic moment indicates existence of half-metal or semiconducting gap, as illustrated in Figs. 2 and 3.

Density of states (DOS) with GGA and GGA + U for ferromagnetic LNMO (001), LNMO (110), and LNMO (111) and LCMO (001), LCMO (110), and LCMO (111) are shown in Figs. 2 and 3, respectively. It is found that below −2 eV, there are mainly O-2*p* states hybridized with *d* states of cations, and above 3 eV, there is a narrow peak of La-*f* states. From −2 eV to 3 eV, there are mainly narrow 3*d* states, in which Co or Ni *d* states are lower than Mn *d* states. *d* states are separated into distinguished t_{2g} and e_g states in strong octahedra crystal field. Furthermore, they are slightly split into five singlet states due to additional weak distortions in *P*21/*n* monoclinic structure. In Fig. 2(f), the total DOS of LNMO (111) FM state shows a gap of 0.4 eV, which is smaller than experimental measurement.[8] In Fig. 3(f), the total DOS of LCMO (111) FM state does not show an insulator gap but is a half-metal. The underestimation of gap size for LNMO and wrong result for LCMO indicates that GGA is not adequate, and electronic correlation effect is crucial. As shown in Figs. 2(e) and 3(e), GGA + U predicts reasonable gaps for both LNMO (111) and LCMO (111) FM states, which are consistent with experiments. The gap value is found to increase more or less linearly upon increasing U value. It is realized that LNMO (111) has a Coulomb-enhanced band gap between fully occupied Ni e_g and empty Mn e_g states in majority spin channel, whereas LCMO (111) has a Hubbard *U* gap caused by electronic correlation in 2/3 occupied Co t_{2_g} states in minority spin channel. Noticeably, the origin of gap in LCMO (111) low-temperature *P*21/*n* monoclinic phase is different from that of high-temperature rhombohedral phase (Space group $R\bar{3}$).[23,24] Moreover, similar results obtained from full-potential linearized augmented plane wave calculations[25] indicate the choice of method does not influence our conclusions.

TABLE I. Total energy (relative to (111) FM state) and total magnetization (moment (μ_B)) of La_2NiMnO_6 and La_2CoMnO_6 per formula unit (*f.u.*).

	Energy	Moment	Energy	Moment
	GGA		GGA + U	
La_2NiMnO_6				
111 (FM)	0	5	0	5
111 (AFM)	0.198	1	0.225	1
001 (FM)	0.473	4.553	0.302	5
001 (AFM)	0.516	0	0.465	0
110 (FM)	0.154	4.729	0.223	5
110 (AFM)	0.155	0	0.247	0
La_2CoMnO_6				
111 (FM)	0	6	0	6
111 (AFM)	0.270	0	0.225	0
001 (FM)	0.188	5.452	0.234	6
001 (AFM)	0.270	1	0.417	1
110 (FM)	0.143	5.237	0.260	6
110 (AFM)	0.184	1	0.261	0

LNMO (001), LNMO (110), LCMO (001), and LCMO (110) are half-metal predicted by GGA + U, as shown in Figs. 2(a), 2(c), 3(a), and 3(c), respectively. The strong on-site repulsion of electrons drives one of the metallic channel insulating, which is different from the cases of LNMO (111) and LCMO (111). LNMO (111) has an electronic configuration of $t_{2g}^{3\uparrow}$ for Mn^{4+} and $t_{2g}^{3\uparrow 3\downarrow}e_g^{2\uparrow}$ for Ni^{2+}, and LCMO (111) has an electronic configuration of $t_{2g}^{3\uparrow}$ for Mn^{4+} and $t_{2g}^{3\uparrow 2\downarrow}e_g^{2\uparrow}$ for Co^{2+}, respectively. However, in the case of (001) and (110) ordering, electron transfers from Ni or Co e_g states to Mn e_g states. The electronic configurations become Mn $t_{2g}^{3\uparrow}e_g^{+\delta\uparrow}$ Ni $t_{2g}^{3\uparrow 3\downarrow}e_g^{2-\delta\uparrow}$ in LNMO and Mn $t_{2g}^{3\uparrow}e_g^{+\delta\uparrow}$ Co $t_{2g}^{3\uparrow 2\downarrow}e_g^{2-\delta\uparrow}$ in LCMO, respectively. The tendency is evident by comparing the magnetic moment per Ni/Mn ion in LNMO, which is 1.37 μ_B/2.95 μ_B in (111), 1.23 μ_B/3.09 μ_B in (110), and 1.13 μ_B/3.20 μ_B in (001), as well as per Co/Mn ion in LCMO, which is 2.46 μ_B/2.82 μ_B in (111), 2.27 μ_B/3.06 μ_B in (110), and 2.20 μ_B/3.12 μ_B in (001). The magnetic moment of Ni and Mn ions in LNMO (111) is very close to previous theoretical results.[12,13] Considering the crystal structure, in LNMO (111), both Mn and Ni ions are linked by six Mn-O-Ni bonding, without Mn-O-Mn and Ni-O-Ni bonding. While in LNMO (110), Mn ion has four Mn-O-Ni plus two Mn-O-Mn bonding whereas Ni ion has four Mn-O-Ni plus two Ni-O-Ni bonding. However, in LNMO (001), Mn ion has two Mn-O-Ni plus four Mn-O-Mn bonding whereas Ni ion has

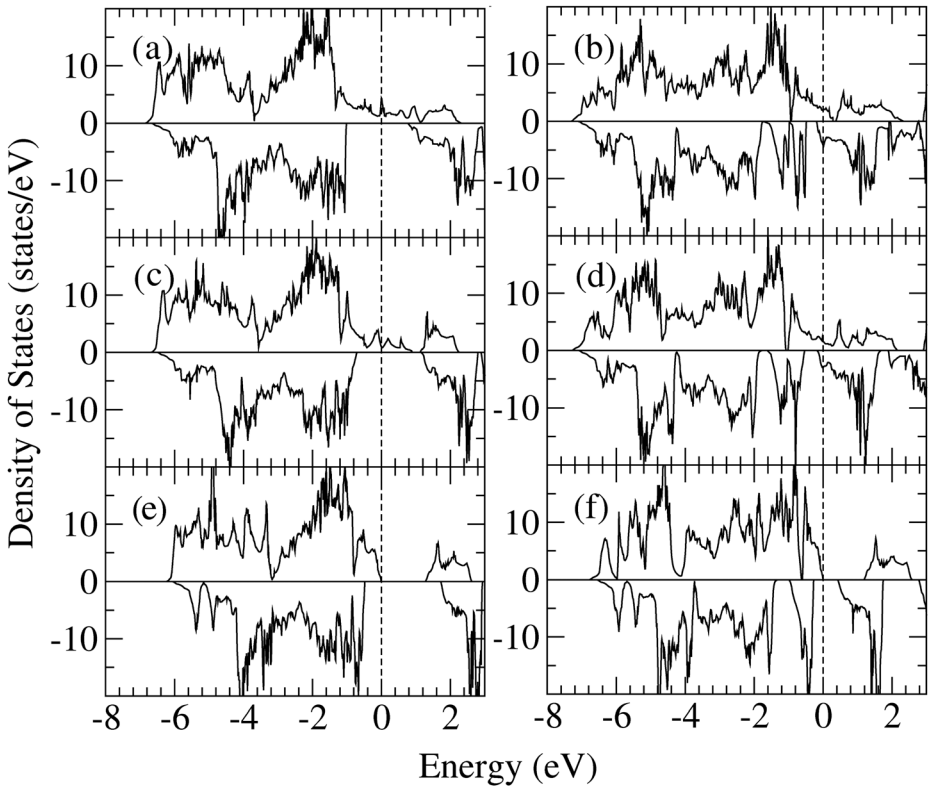

FIG. 2. DOS of ferromagnetic La_2NiMnO_6 with different Ni/Mn orders: (a) (001) order with GGA + U, (b) (001) order with GGA, (c) (110) order with GGA + U, (d) (110) order with GGA, (e) (111) order with GGA + U, and (f) (111) order with GGA.

two Mn-O-Ni plus four Ni-O-Ni bonding. Similar variations of bonding could also be found in LCMO. Additional Mn-O-Mn, Ni-O-Ni, or Co-O-Co bonding expands e_g states, which results in the partial occupied e_g states of Mn, Ni, and Co in majority spin channel. Thus, the half-metallic property occurs as on-site U induces a gap in minority spin channel.

In the superlattice with (001) and (110) cationic ordering, the valence state seems to be between 4+ and 3+ for Mn ions whereas between 2+ and 3+ for Ni or Co ions. It is different from Mn^{3+}/Ni^{3+} or Mn^{3+}/Co^{3+} pairs expected in disorder phase.[8,9,16] According to Goodenough-Kanamori rules,[26,27] Mn^{4+}-O-Ni^{2+} or Mn^{4+}-O-Co^{2+} has FM exchange interaction,

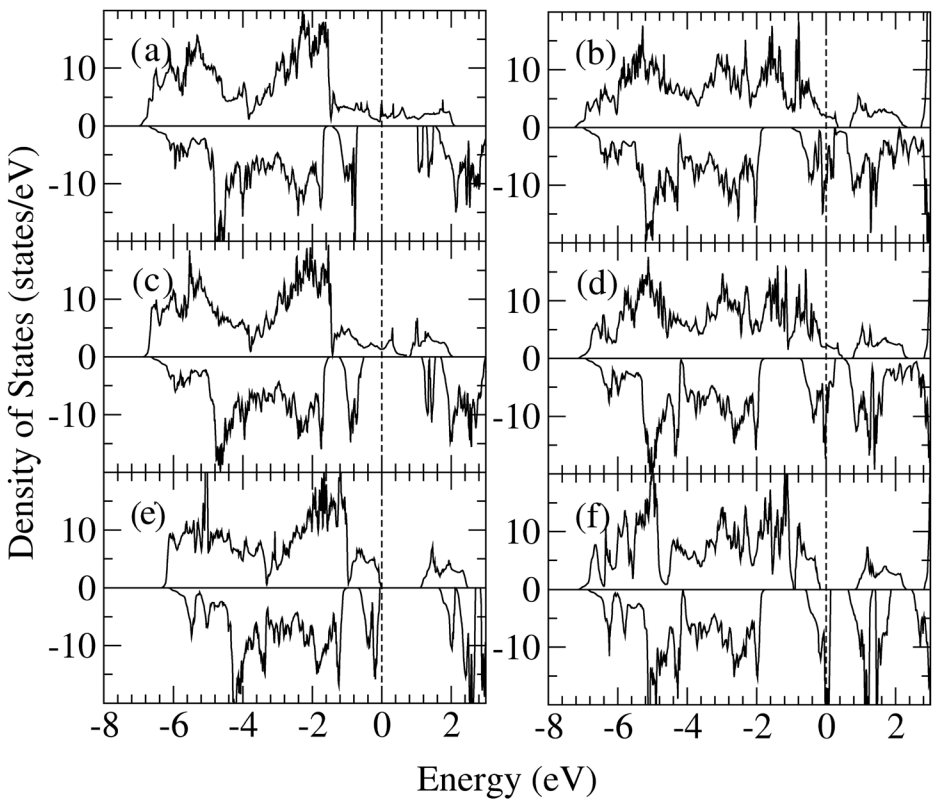

FIG. 3. DOS of ferromagnetic La_2CoMnO_6 with different Co/Mn orders: (a) (001) order with GGA + U, (b) (001) order with GGA, (c) (110) order with GGA + U, (d) (110) order with GGA, (e) (111) order with GGA + U, and (f) (111) order with GGA.

while Mn^{3+}-O-Ni^{3+} or Mn^{3+}-O-Co^{3+} has AFM exchange interaction. For the middle valence state, our calculations reveal that $Mn^{(4-\delta)+}$-O-Ni $^{(2+\delta)+}$ or $Mn^{(4-\delta)+}$-O-$Co^{(2+\delta)+}$ has FM exchange interaction in either GGA or GGA + U, although being a tendency to AFM.

In summary, our calculations indicate that LNMO (001), LNMO (110), LCMO (001), and LCMO (110) should be ferromagnetic half-metal, while LNMO (111) and LCMO (111) are ferromagnetic semiconductors with a Coulomb-enhanced band gap and a Hubbard *U* gap, respectively. As the cationic ordering has significant influence, it could be, therefore, meaningful to explore the cationic ordering effect in more perovskite oxides.

This work is supported by Nature Science Foundation of China (Grant No. 10704024), by Shanghai Rising-Star Program (Grant No. 08QA14026), and by Shanghai Scientific Project (Grant No. 08JC1408400).

[1]S. A. Wolf, D. D. Awschalom, R. A. Buhrman, J. M. Daughton, S. von Molnar, M. L. Roukes, A. Y. Chtchelkanova, and D. M. Treger, Science **294**, 1488 (2001).
[2]D. D. Awschalom, M. E. Flatte, and N. Samarth, Sci. Am. **286**, 66 (2002).
[3]N. S. Rogado, J. Li, A. W. Sleight, and M. A. Subramanian, Adv. Mater. **17**, 2225 (2005).
[4]Y. Q. Lin and X. M. Chen, J. Am. Ceram. Soc. **94**, 782 (2011).
[5]M. W. Lufaso and P. M. Woodward, Acta Cryst. B **60**, 10 (2004).
[6]C. L. Bull and P. F. McMillan, J. Solid State Chem. **177**, 2323 (2004).
[7]J. B. Goodenough, A. Wold, R. J. Arnott, and N. Menyuk, Phys. Rev. **124**, 373 (1961).
[8]R. I. Dass, J. Q. Yan, and J. B. Goodenough, Phys. Rev. B **68**, 064415 (2003).
[9]R. I. Dass and J. B. Goodenough, Phys. Rev. B **67**, 014401 (2003).
[10]C. L. Bull, D. Gleeson, and K. S. Knight, J. Phys. Condens. Matter **15**, 4927 (2003).
[11]S. F. Matar, M. A. Subramanian, A. Villesuzanne, V. Eyert, and M.-H. Whangbo, J. Magn. Magn. Mater. **308**, 116 (2007).
[12]B. Kim, J. Lee, B. Hyun Kim, H. C. Choi, K. Kim, J.-S. Kang, and B. I. Min, J. Appl. Phys. **105**, 07E515 (2009).
[13]H. Das, U. V. Waghmare, T. Saha-Dasgupta, and D. D. Sarma, Phys. Rev. Lett. **100**, 186402 (2008).
[14]H. Guo, J. Burgess, S. Street, A. Gupta, T. G. Calvarese, and M. A. Subramanian, Appl. Phys. Lett. **89**, 022509 (2006).
[15]H. Z. Guo, J. Burgess, E. Ada, S. Street, A. Gupta, M. N. Iliev, A. J. Kellock, C. Magen, M. Varela, and S. J. Pennycook, Phys. Rev. B **77**, 174423 (2008).
[16]M. P. Singh, K. D. Truong, S. Jandl, and P. Fournier, Phys. Rev. B **79**, 224421 (2009).
[17]H. Z. Guo, A. Gupta, M. Varela, S. Pennycook, and J. D. Zhang, Phys. Rev. B **79**, 172402 (2009).
[18]S. Budak, C. Muntele, I. Muntele, H. Guo, A. Gupta, and D. Ila, Nucl. Instrum. Methods Phys. Res. B **261**, 686 (2007).
[19]M. N. Iliev, M. V. Abrashev, A. P. Litvinchuk, V. G. Hadjiev, H. Guo, and A. Gupta, Phys. Rev. B **75**, 104118 (2007).
[20]G. Kresse and J. Furthmuller, Phys. Rev. B **54**, 11169 (1996).
[21]J. P. Perdew, K. Burke, and M. Ernzerhof, Phys. Rev. Lett. **77**, 3865 (1996).
[22]P. E. Blochl, Phys. Rev. B **50**, 17953 (1994).
[23]The rhombohedral phase has doubly degenerate e_g^{π} and e_g^{σ} states, which results in the half-metallic properties within GGA + U. The insulating gap is driven by Coulomb-assisted spin-orbit coupling (see details in Ref. 24), while the d states of monoclinic phase has five singlets so that on-site Coulomb repulsion could open a gap.
[24]S. Baidya and T. Saha-Dasgupta, Phys. Rev. B **84**, 035131 (2011).
[25]P. Blaha, K. Schwzrz, G. K. H. Madsen, D. Kvasnicka, and J. Luitz, *WIEN2K, An Augmented Plane Wave+Local Orbitals Program for Calculating Crystal Properties* (Technical University Wien, Austria, 2001).
[26]J. B. Goodenough, Phys. Rev. **100**, 564 (1955).
[27]J. Kanamori, J. Phys. Chem. Solids **10**, 87 (1959).